

ESTIMATION OF VELOCITY, SHAPE, AND POSITION
OF MOVING OBJECTS WITH SAR *

Martin Kirscht

Institut für Theoretische Nachrichtentechnik und Informationsverarbeitung, Universität Hannover
Appelstr. 9A, D-30167 Hannover, Germany
Phone: +49 511 762-5305, Fax: +49 511 762-5333, E-mail: kirscht@tnt.uni-hannover.de,
<http://www.tnt.uni-hannover.de/~kirscht>

ABSTRACT

In synthetic aperture radar (SAR) images, moving objects appear defocused or at wrong positions, depending on the direction of their motion. In order to get a correct and focused image of the moving objects, it is necessary to know the real positions and velocities of the objects. Here, a method for detection of arbitrarily moving ground-based objects and for estimation of their velocities, shapes, and positions is presented. The knowledge of these parameters is used to compensate the SAR image, i. e. to eliminate the imaging errors due to object motion. The proposed method is based on evaluation of a sequence of single-look SAR images, generated from conventional SAR raw data. It is shown that the knowledge of the shapes of the objects can improve the compensation of the SAR image. Two kinds of imaging of the moving objects including the stationary background are possible, either in a compensated multilook image or in a compensated sequence of single-look images.

1.0 INTRODUCTION

In synthetic aperture radar (SAR) images, ground moving objects appear defocused or at wrong positions depending on the direction of the object motion. An object moving linearly in along-track (azimuth) direction causes a blurring in azimuth direction whereas an object moving in cross-track (range) direction causes mainly a displacement in azimuth direction. These imaging errors can be compensated for by detecting the moving objects, estimating their velocities and positions, and compensating for their motion.

For detection of moving objects and for moving target imaging (MTI) a number of algorithms have been proposed. They usually work on range compressed SAR raw data, either transformed to the Doppler frequency domain (e. g. Freeman, 1987, D'Addio, 1994), to a time-frequency domain (Barbarossa, 1992) or to a Doppler-rate map (Moreira, 1995). Freeman and Currie proposed a division of the Doppler spectrum into four bands, where one band contains the clutter (i. e. the stationary background) and the other ones the range moving objects. Either a conventional SAR image or images of the moving objects can be generated. Chen and McGillem additionally compensate the range velocity component by shifting the spectra of the objects towards the clutter spectrum. In the SAR image the range moving objects appear at the correct positions provided that the antenna beamwidth is small (Chen, 1992). A restriction of these algorithms is that the pulse repetition frequency (PRF) has to be at least four times higher than the Doppler bandwidth of the clutter. To fulfill this condition, either the clutter bandwidth and concurrently the resolution in azimuth

* Presented at the Fourth International Airborne Remote Sensing Conference and Exhibition / 21st Canadian Symposium on Remote Sensing, Ottawa, Ontario, Canada, 21-24 June 1999.

direction has to be reduced as done in (Chen, 1992), or the PRF has to be increased with the disadvantage of a more complex SAR system. However, the detection of objects with an azimuth velocity component only is not possible by applying these algorithms. Another way is to calculate a Doppler rate map from the range compressed data and to estimate the azimuth velocity component from the Doppler rate and the range velocity component from the range migration as shown in (Moreira, 1995). This algorithm has the restriction to be partly interactive and to be able to detect only moving objects whose Doppler rate differs significantly from that of the clutter. This means that slowly moving objects cannot be detected.

In this paper, a method for detection of moving objects, for estimation of their velocities, shapes, and positions, and for compensation of the imaging errors is presented. This method is based on the evaluation of a sequence of single-look SAR images, which are generated from conventional SAR raw data. Compared to the algorithms (Freeman, 1987) and (Barbarossa, 1992), the proposed algorithm has the advantage that also objects moving mainly in azimuth direction can be detected and that the PRF needs to be only a little higher than the clutter bandwidth. The better sensibility to slowly moving objects and the capability of compensating the imaging errors are advantages when compared to (Moreira, 1995). Compared to an earlier version of this algorithm (Kirscht, 1998), the estimation of the range velocity component has been improved and the estimation of the shapes of moving objects has been added in order to improve the imaging of the moving objects.

The proposed algorithm consists of three main steps as shown in Fig. 1. The first step is the generation of a sequence of single-look SAR images. Afterwards, the detection and parameter estimation of moving objects follows. It consists of the detection of candidates, the velocity estimation, the verification of the candidates, and the estimation of shape and position. The third step is the compensation of the object motion and the imaging of the moving objects. Two kinds of imaging of the moving objects are possible, either in a multilook image or in a compensated sequence of single-look images. The multilook image shows the moving objects overlaid on the clutter background and provides a high quality with regard to speckle noise. The latter possibility allows to visualize the object motion. The following chapters of the paper describe the several steps of the algorithm. The paper finishes with experimental results and a conclusion.

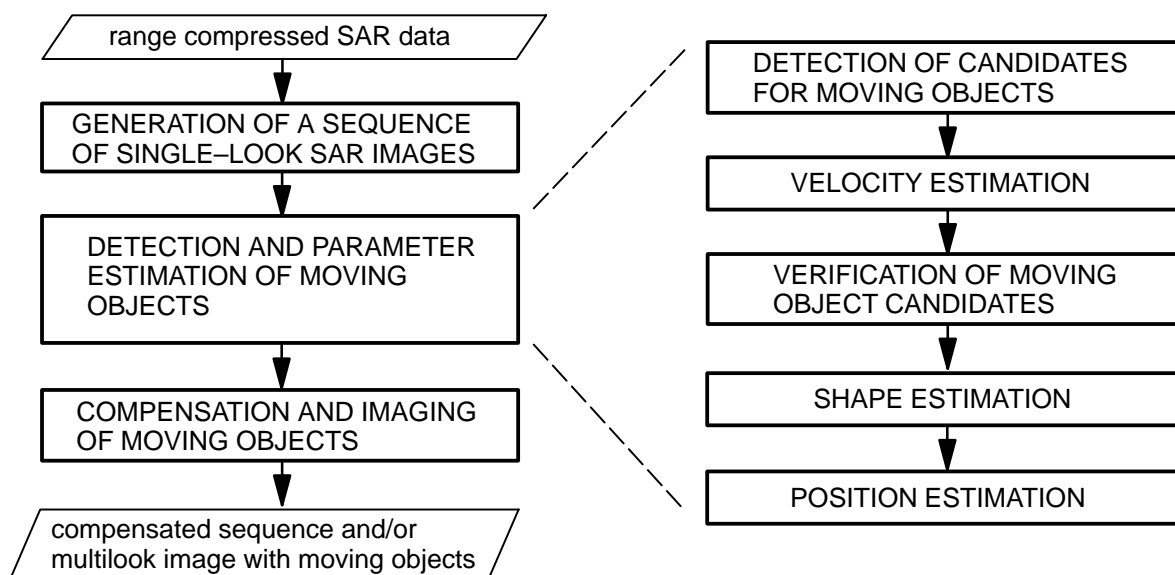


Figure 1. Block diagram of the proposed algorithm

2.0 GENERATION OF A SEQUENCE OF SINGLE-LOOK SAR IMAGES

The sequence of SAR images is generated from single-channel, i. e. conventional SAR raw data by processing images using data from various frequency bands out of the complete Doppler spectrum. Each image i shows the ground at a specific (azimuth) look angle

$$\theta_i = - \arcsin \frac{f_{l_i} \lambda}{2 v_{Ax}} \quad (1)$$

depending on the look center frequency f_{l_i} . The images are therefore called single-look images. In Eq. (1), λ and v_{Ax} denote the carrier wavelength and the antenna speed in azimuth direction x , respectively. For static objects the different look angles θ_i correspond with different times

$$t_i \approx t_0 + \frac{\theta_i R_{T_0}}{v_{Ax}} \approx t_0 - \frac{f_{l_i} \lambda R_{T_0}}{2 v_{Ax}^2} \quad \text{for } \sin \theta_i \ll 1 \quad (2)$$

where R_{T_0} is the minimal distance between antenna and object and t_0 is an initial time.

In order to get a geometrically correct and static background in the images of the sequence, a ground range projection and a range migration correction is performed. In this manner we get a sequence of consecutive images where the stationary background remains at the same position, whereas the positions of the moving objects change from image to image. Therefore, the motion of the moving objects can be observed.

3.0 DETECTION AND PARAMETER ESTIMATION OF MOVING OBJECTS

The detection and parameter estimation algorithm consists of five steps. In the first step candidates for moving objects are detected and in the second step a velocity estimation is performed for each candidate. Afterwards the candidates are verified to be moving objects and their shape and position is estimated.

3.1 DETECTION OF CANDIDATES FOR MOVING OBJECTS

The velocity estimation described in the next section will be done for each moving object individually. As no moving objects have been detected so far, candidates for moving objects are detected first. This is done by searching for small regions with a locally high signal amplitude. The signal amplitude in a SAR image is a measure for the radar cross section (RCS). Due to the metallic surface of moving objects their RCS is assumed to be higher than the surrounding. By reason of plausibility, the maximum allowed number of pixels of a candidate is limited which reduces the number of candidates.

3.2 VELOCITY ESTIMATION

The object velocity is a vector with two components, one in azimuth direction and one in range direction. The velocity of a moving object candidate is obtained by estimating their displacement vectors, which give the displacement of the candidate in pairs of two successive images of the generated sequence. The displacement vector is obtained using a modified block matching algorithm (Bierling, 1988). This algorithm searches for the best match between blocks in two successive images with regard to the normalized cross correlation function as matching criterion. In the second of a pair of images the block is set centered around a candidate. Then in the previous image that position is searched which leads to the maximum correlation between the two blocks. The difference of the positions is taken as displacement vector. It is measured in the unit pixel per image. This displacement vector is then used to calculate the velocity components.

3.2.1 Estimation of the azimuth velocity component

In (Kirscht, 1997), it has been shown that the azimuth component of the object velocity can be estimated from the azimuth component of the displacement vector Δx as

$$\hat{v}_{Tx} = v_{Ax} \cdot \left[1 - \left(1 - \frac{2 \Delta x \delta x v_{Ax}}{\Delta f_l \lambda R_{T_0}} \right)^{-\frac{1}{2}} \right] \quad \text{for } \frac{\Delta x \delta x}{\Delta t} > -v_{Ax}, \quad (3)$$

where δx is the pixel spacing in azimuth direction and Δf_l is the difference between the look center frequencies of two successive images. The time difference Δt between two successive images is given by

$$\Delta t = t_i - t_{i-1} \approx \frac{\Delta \theta R_{T_0}}{v_{Ax}} \approx -\frac{\Delta f_l \lambda R_{T_0}}{2v_{Ax}^2} \quad \text{for } \sin \theta \ll 1, \quad (4)$$

where $\Delta \theta = \theta_i - \theta_{i-1}$ is the difference between the look angles of two images. Eq. (3) is an enhanced version of

$$\hat{v}_{Tx} \approx \frac{\Delta x \delta x}{2\Delta t} = -\frac{\Delta x \delta x v_{Ax}^2}{\Delta f_l \lambda R_{T_0}}, \quad (5)$$

which is only valid for small object velocities $|v_{Tx}| \ll v_{Ax}$. The left side of Eq. (5) has been shown in (Ouchi, 1985), where the right side is added here to show the relation to Eq. (3).

3.2.2 Estimation of the range velocity component

Only a small part of the object motion in range direction is contained in the measured displacement vector component Δy . This is because the range positions of objects with a non-zero range velocity component are not correct due to the range migration correction. On the other hand, range migration correction is necessary to get a static background. To get an accurate estimate \hat{v}_{Ty} of the range velocity component the displacement of a static object due to range migration is considered. Between two successive images the position of the antenna changes by

$$\Delta x_A = \Delta t v_{Ax} \quad (6)$$

and the distance between antenna and object changes by

$$\Delta R_{T_0}(t) = \sqrt{x_A(t)^2 + R_{T_0}^2} \pm \sqrt{(x_A(t) + \Delta x_A)^2 + R_{T_0}^2}, \quad (7)$$

where $x_A(t)$ is the antenna position in the first of the two considered images and $x_A(t_0) = 0$ is the position when the object is broadside the airplane. The sign depends on whether the object is in front of or behind the airplane. From Eq. (6) and (7) one gets the displacement of the clutter in range direction in the unit [pixel per image] as

$$\Delta v_{cl}(t) = \frac{\Delta R_{T_0}(t) \sin \gamma}{\delta x} \approx \frac{\sin \gamma}{\delta x} \cdot \left[\sqrt{x_A(t)^2 + R_{T_0}^2} \pm \sqrt{\left(x_A(t) - \frac{\Delta f_l \lambda R_{T_0}}{2v_{Ax}} \right)^2 + R_{T_0}^2} \right], \quad (8)$$

with γ the incidence angle or ($90^\circ - \text{depression angle}$). Finally, an estimate for the range velocity component in [m/s] is calculated from the displacement vector component $\Delta y(t)$ according to

$$\hat{v}_{Ty}(t) = \frac{[\Delta y(t) - \Delta y_{cl}(t)] \delta x}{\Delta t}. \quad (9)$$

3.3 VERIFICATION OF MOVING OBJECT CANDIDATES

The candidates are tracked from image to image according to their estimated displacement vectors. If the estimated velocities are non-zero and remain nearly constant during a fixed number of images, the candidate will be verified to be a moving object. Thus, static candidates are sorted out. In order to get a reliable velocity, the velocity estimates according to Eq. (3) and (9) from successive image pairs are averaged.

3.4 SHAPE ESTIMATION

The shape of a moving object which can be observed in a single-look SAR image is not the real shape but a blurred one. The blurring of this observed shape depends on the look bandwidth of the image. If it is small, the observation interval is very short and therefore the observed shape will coincide with the real shape of the object. On the other hand, the disadvantage of a small look bandwidth is a decreased resolution in azimuth direction. Therefore, the choice of the look bandwidth is a compromise between these two effects and the real shape of an object can only be obtained from the observed shape directly for low object velocities. Provided that the frequency bands of the images do not overlap, the look bandwidth is equal to the distance between two successive look center frequencies. This also means that for a point-like object the observed shapes in two successive single-look images are nearly adjacent. The overlapping of the observed shapes in two successive images is therefore a measure for the real shape of an object.

In general, the observed shape is obtained as follows. Beginning at the pixel with the highest amplitude, a closed area around the center pixel is created. The border of this closed area is set to the location where the gradient of the image amplitudes in radial direction relative to the center pixel is maximal. An estimate for the real shape is obtained by shrinking the observed shape in azimuth direction in order to match the mentioned overlapping area.

3.5 POSITION ESTIMATION

For the compensation of the imaging errors also the position of a moving object has to be estimated. This position is called 'reference position' and is attained when the object is broadside the airplane, i. e. in the center of the antenna beam. It is calculated by averaging the positions obtained from the images of the sequence. Additionally the estimated range velocity component requires a correction of the azimuth position by

$$\Delta x = \frac{\hat{v}_{Ty} \sin \gamma}{v_{Ax}} \cdot R_{T_0}, \quad (10)$$

which arises due to the additional Doppler shift

$$f_{D_{Tc}} = - \frac{2v_{Ty} \sin \gamma}{\lambda} \quad (11)$$

inherent to the return signals of an object moving in range direction.

To get a more accurate position in azimuth direction, also the signal amplitude of an object in the several images of the sequence is considered. It is assumed that the signal amplitude is maximal when the object is in the center of the antenna beam. The corresponding image is that one with a look center frequency close to the Doppler shift from Eq. (11). Vice versa, a Doppler shift can be estimated from the 'center of gravity' of the signal amplitudes. If the range velocity estimated from this Doppler shift, using Eq. (11), does not coincide with that one from Eq. (9), the azimuth position will be adjusted in order to minimize the difference between these velocities.

4.0 COMPENSATION AND IMAGING OF MOVING OBJECTS

The aim of the compensation of the imaging errors is to get a focused image of moving objects and the static background on the one hand, and a compensated sequence of single-look images on the other hand. In both image products the objects should appear at the correct positions. For the first possibility the compensation is done by shifting each moving object to the reference position in each image of the sequence, using the previously estimated shape. In case of range moving objects also the fact that an object appears earlier or later in the sequence according to

$$\Delta t_T = - \frac{f_{D_{Tc}} \lambda R_{T_0}}{2v_{Ax}^2} \quad (12)$$

is considered by shifting the objects in temporal direction, also. By averaging the middle images of the sequence centered around the image with a look center frequency similar to the mean Doppler frequency one gets a compensated multilook image where the moving objects appear focused at the reference position.

The second imaging possibility is to recalculate the positions of the objects in the sequence according to the reference position and the estimated velocity components. A compensated sequence is obtained by eliminating the moving objects from their original positions and inserting them at the recalculated positions. This yields a sequence where the motion of the objects is visible but the objects appear nearly at the correct positions.

5.0 RESULTS

The proposed algorithm has been applied to simulated and to real raw data successfully. A PRF of two times the clutter bandwidth has been used. The simulated data have been used to verify the estimation accuracy of the algorithm. Simulated data are generated by simulating raw data of 15 moving objects with different velocities and superimposing them on real clutter data. Fig. 2 shows a sample image out of a representative sequence. Most of the objects originally drive on the road whereas two objects in the lower part of the image drive on the runway of the airport. The objects appear no longer on the road but are shifted in azimuth direction due to the different range velocity components. Fig. 3 shows an image from the compensated sequence. The moving objects now appear again on or near the road at their correct positions.

In Fig. 4, a multilook image, the common output of a SAR processor, is shown using the same data as in Fig. 2. The moving objects appear blurred and shifted. After the compensation of the imaging errors and the averaging of the single-look images a compensated multilook image as shown in Fig. 5 is obtained. The displacement and blurring of all objects is compensated. The moving objects are displayed nearly at their real positions.

By applying the algorithm to simulated data, the mean standard deviation of the error of the azimuth velocity estimates is 2.8 km/h (0.78 m/s) for an azimuth velocity component of up to 80 km/h and a range velocity component of up to 50 km/h. The standard deviation of the error of the range velocity estimates is 9.9 km/h (2.7 m/s) for range velocities of up to 75 km/h. This value is less accurate than that for the azimuth component due to the fact that quickly moving objects can sometimes not be tracked during the whole sequence. If for instance one object is detected as two ones in two consecutive sets of images, the time shifts and the estimated Doppler shifts according to Eq. (11) will differ from the real values. Supposition for a detection is a minimal azimuth component of 5 km/h or a range component of 20 km/h. In case of the presence of both components the lower bound for the range component decreases towards 0 km/h. The position is estimated with a mean standard deviation of the position error of 34 m in azimuth and 2.9 m in range direction.



Figure 2. Single-look image from a sequence generated from simulated raw data of 15 moving objects superimposed on real clutter data; Detected moving objects are marked;

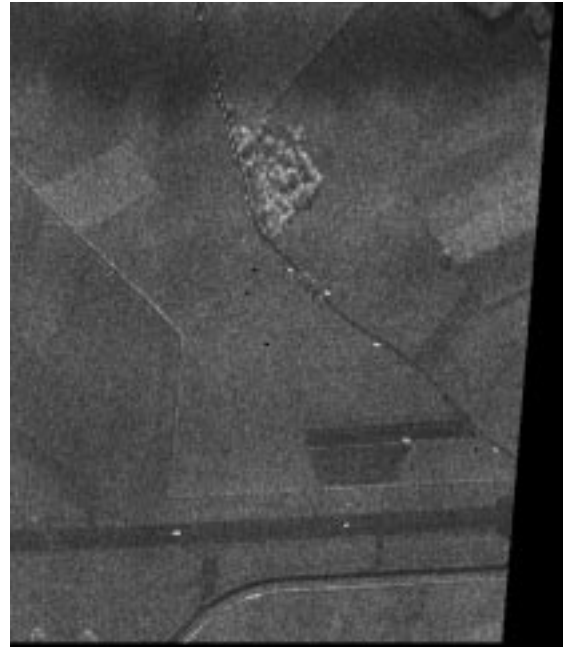


Figure 3. Single-look image from the compensated sequence (same data as in Fig. 2); The moving objects are now located near their real positions on the road or on the runway;



Figure 4. Multilook image generated from the same data as in Fig. 2, using a conventional SAR processor; the moving objects appear blurred and shifted or are even disappeared

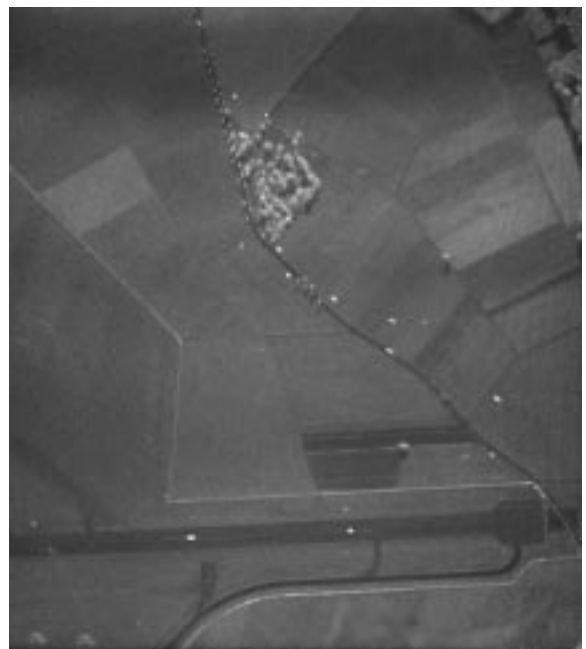


Figure 5. Compensated multilook image; all moving objects have been detected and compensated and appear focused near the real positions on the road and the runway, respectively

6.0 CONCLUSIONS

In this paper, a method for detection of moving objects and for estimation of their parameters velocity, shape, and position has been presented. The knowledge of these parameters has been used to compensate for the imaging errors of the object motion. The method evaluates a sequence of single-look SAR images, generated from conventional SAR raw data. These images show the ground at different look angles and therefore at different times. By tracking the objects from image to image and by evaluating the change in position and the signal amplitude, the object velocities are estimated with a mean standard deviation of the error of 2.8 km/h and 9.9 km/h for the azimuth and range component, respectively. The position is estimated with a mean standard deviation of the position error of 34 m and 2.9 m in azimuth and range direction, respectively. It has been shown that with the knowledge of the shape either a compensated multilook image or a compensated sequence can be generated where the moving objects appear focused and at the estimated positions. In the compensated sequence the motion of the objects is visible.

The advantages of the method are the toleration of a small PRF and the capability of detecting slowly moving objects as well as other moving objects nearly independent of their motion direction.

7.0 ACKNOWLEDGMENTS

This work was supported by the German Federal Government. The author thanks DASA Dornier, Friedrichshafen, Germany, for providing the SAR raw data.

8.0 REFERENCES

- E. D'Addio, M. Di Bisceglie, and S. Bottalico, "Detection of moving objects with airborne SAR." *Signal Processing (Eurasip)*, Vol. 36, No. 2, pp. 149–162, March 1994.
- S. Barbarossa and A. Farina: "Detection and imaging of moving objects with synthetic aperture radar, Part 2: Joint time–frequency analysis by Wigner–Ville distribution." In *IEE Proceedings–F*, Vol. 139, No. 1, pp. 89–97, Feb. 1992.
- M. Bierling, "Displacement estimation by hierarchical blockmatching." In *Proc. 3rd SPIE Symposium on Visual Communications and Image Processing*, Cambridge, USA, pp. 942–951, 1988.
- H. Chen and C. McGillem, "Target motion compensation by spectrum shifting in SAR." *IEEE Trans. Aerospace and Electronic Systems*, Vol. 28, No. 3, pp. 895–901, July 1992.
- A. Freeman and A. Currie, "Synthetic aperture radar (SAR) images of moving targets." *GEC Journal of Research*, Vol. 5, No. 2, pp. 106–115, 1987.
- M. Kirscht, "Detection and focused imaging of moving objects evaluating a sequence of single-look SAR images." In *Proc. of the Third International Airborne Remote Sensing Conference and Exhibition*, Copenhagen, Denmark, Vol. I, pp. 393–400, July 1997.
- M. Kirscht, "Detection, velocity estimation and imaging of moving targets with single-channel SAR." In *Proc. of European Conference on Synthetic Aperture Radar, EUSAR '98*, Friedrichshafen, Germany, pp. 587–590, May 1998.
- J. R. Moreira and W. Keydel, "A new MTI–SAR approach using the reflectivity displacement method." *IEEE Trans. Geoscience and Remote Sensing*, Vol. 33, No. 5, pp. 1238–1244, Sept. 1995.
- K. Ouchi, "On the multilook images of moving targets by synthetic aperture radars." *IEEE Trans. Antennas and Propagation*, Vol. AP–33, No.8, pp. 823–827, 1985.
- R. K. Raney, "Synthetic aperture imaging radar and moving targets." *IEEE Trans. Aerospace and Electronic Systems*, Vol. AES–7, No. 3, pp. 499–505, May 1971.